PAPER • OPEN ACCESS

Molecular-frame photoelectron angular distributions during double core-hole generation in O_2 and N_2 molecules

To cite this article: Dmitrii V Rezvan *et al* 2023 *J. Phys. B: At. Mol. Opt. Phys.* **56** 195003

View the article online for updates and enhancements.

Molecular-frame photoelectron angular distributions during double core-hole generation in O_2 and N_2 molecules

Dmitrii V Rezvan[1] [iD], **Nikolay M Novikovskiy[1]** [iD], **Daniel M Haubenreißer[1]**,
Boris M Lagutin[2] [iD] **and Philipp V Demekhin[1],*** [iD]

[1] Institut für Physik und CINSaT, Universität Kassel, Heinrich-Plett-Straße 40, 34132 Kassel, Germany
[2] Rostov State Transport University, Narodnogo Opolcheniya Square 2, 344038 Rostov-on-Don, Russia

E-mail: demekhin@physik.uni-kassel.de

CrossMark

Abstract

Angular distributions of photoelectrons emitted upon double core-hole (DCH) generation in nitrogen and oxygen molecules are studied theoretically in the frame of a molecular reference. The respective electronic structure calculations are performed by the single center method for photoelectron kinetic energies up to 40 eV in the relaxed-core Hartree–Fock approximation. The molecular frame photoelectron angular distributions are computed for single-site and two-site DCH creation processes and further analyzed for different orientations of the molecular axis with respect to the electric field vector of linearly polarized incident light and for localized or delocalized emitting atomic site scenarios. The present theoretical results provide reliable predictions for future experiments with high-repetition free-electron lasers.

Keywords: photon interactions with molecules, inner-shell photoionization, double core-hole generation, molecular-frame angular distributions

(Some figures may appear in colour only in the online journal)

1. Introduction

The site- and emitter-selectivity of a core-hole spectroscopy promoted it to one of the standard tools for exploring the nearest chemical environment in molecules with the help of synchrotron radiation [1]. About 35 years ago, it was proposed theoretically that creating double core-hole (DCH) states, i.e. states where two core-electrons are simultaneously missing, provides a more sensitive tool for probing chemical environment in molecules [2, 3]. This gave impetus to subsequent theoretical investigations of properties of the DCH states [4–6]. The DCH states can be generated by a two-photon double-ionization, which suggests that a molecule sequentially absorbs two high-energy photons on a relaxation timescale of the primary core-hole state (typically few femtoseconds). Since this is a rather unlikely process, its observation requires considerably larger photon fluxes that can be provided by synchrotron radiation facilities [7]. Therefore, DCH states were first observed with the help of third-generation synchrotron radiation sources via an alternative, higher-order mechanism of a double core–shell ionization by a single high-energy photon that carried sufficient energy [8–11].

The advent of x-ray free-electron lasers (XFELs), which provide sufficient photon flux to trigger DCH states via the ultrafast sequential two-photon double-ionization, stimulated further theoretical [12–15] and experimental [16–20] studies of the DCH states. Of particular importance for the present work, is the very recent study of the DCH generation in O_2 molecules [20]. By performing a coincident

---

* Author to whom any correspondence should be addressed.

detection of charged particles, and also owing to a high repetition rate of the European XFEL, the authors were able to access molecular-frame photoelectron angular distributions (MFPADs) for the second emission step and compare those distributions for the two types of states, where both core-holes were created on a single-site (ss-DCH) or on two-sites (ts-DCH) of a molecule. The MFPADs, are known to be very sensitive to each detail of the molecular potential [21–24]. Surprisingly, a difference between the polarization-averaged emission distributions (PA-MFPADs), observed for the ss-DCH and ts-DCH states, was rather marginal, and this was also confirmed by the accompanying theory.

Since the DCH states in O_2 were created in [20] at different, relatively high, photoelectron kinetic energies (i.e. at 30 eV for the ss-DCH and at 110 eV for the ts-DCH photoelectrons, both generated at the same photon energy of 670 eV), the authors suggested to compare MFPADs for much lower and equal photoelectron kinetic energies. In addition, it was proposed to further differentiate the data by considering a situation of emission of the secondary photoelectron from only one of the oxygen atoms in the homonuclear O_2 molecule (localized emitting site scenario), as well as choosing particular orientations of the light polarization with respect to a molecular axis (parallel or perpendicular for the used linearly polarized light). In the present work, we perform a systematic theoretical study of the MFPADs of secondary photoelectrons with the kinetic energies below 40 eV, which are emitted during the DCH generation processes in homonuclear O_2 and N_2 molecules. The present analysis is performed along the lines proposed in [20] (see above). Our theoretical approach is outlined in section 2, while the presently obtained results are presented and discussed in section 3. We conclude with a brief summary in section 4.

2. Theory

Let us define an orientation of the axis of a linear molecule (molecular z_M-axis) with respect to the electric field vector of linearly polarized light (laboratory z_L-axis) by the Euler angle β (the other two Euler angles are irrelevant here and can be set to $\alpha = \gamma = 0$), and the photoelectron emission in the molecular frame of reference by spherical angles θ and φ. In this case, the total amplitude for the emission of a photoelectron of energy $\varepsilon = k^2/2$ with the momentum vector $\vec{k} = \{k, \theta, \varphi\}$ is given by [25–28]

$$T_\varepsilon (\beta, \theta) = \sum_{\ell m k} (-i)^\ell D_{k0}^1 (\alpha, \beta, \gamma) A_{\varepsilon \ell m k} Y_{\ell m} (\theta, \varphi), \quad (1)$$

where $\mathcal{D}_{k0}^1$ are the Wigner rotation matrices, and $Y_{\ell m}$ spherical functions. If we consider the polarization plane to be the molecular xz_M-plane, then the azimuthal photoemission angle needs to be set to $\varphi = 0$ and $\varphi = \pi$ for $x_M > 0$ and $x_M < 0$ hemiplanes, respectively. The transition amplitude (1) provides an access to the MFPADs via

$$\sigma_\varepsilon (\beta, \theta) = |T_\varepsilon (\beta, \theta)|^2. \quad (2)$$

Apart from the geometry details of the process discussed above, a complete information on the photoionization process and on the molecule itself is contained in the quantities $A_{\varepsilon \ell m k}$, which are the molecular-frame dipole transition amplitudes for the emission of partial photoelectron continuum waves with angular momentum ℓ and its projection m caused by the absorption of a photon of polarization k. In the present work, these amplitudes were computed with the stationary single center (SC) method [29–32], which was successfully applied in the past to study angle-resolved inner-shell photoionization of the O_2 [20, 26, 33] and N_2 [28, 34, 35] molecules. The present calculations were performed at the equilibrium geometry of the neutral molecules using the SC expansions of molecular orbitals for the bound and continuum electrons over the partial spherical harmonics with maximal orbital momenta $\ell_{\text{bound}} \leqslant 99$ and $\ell_{\text{cont}} \leqslant 49$, respectively. As was demonstrated in our previous work on the DCH generation in O_2 [20], it is important here to account for the core-relaxation effects during the second photoionization step (see figure 2(a) there). There, a broad σ-shape resonance emerged in the photoelectron energy range of the ss-DCH in the frozen-core Hartree–Fock approximation, and this one-particle approximation therefore failed. Therefore, the present calculations were performed in the relaxed-core Hartree–Fock approximation (RCHF), in which the initial bound molecular orbitals were computed in configurations of the K^{-1} single core-hole states, while the final bound orbitals, which generate a molecular potential for the photoelectron in continuum, were obtained in respective configurations of the $K^{-1}K^{-1}$ or KK^{-2} DCH states. Extended investigations yielded that using the RCHF approximation guarantees an absence of shape resonances in the considered photoelectron energy range for both molecules.

3. Results and discussion

We first consider a situation from the experiment of [20], where an emitting site of the O_2 molecule was not resolved, and the respective MFPADs represent the secondary photoemission from two identical atoms in a homonuclear molecule on average (i.e. when emitting site of the second photoelectron is not resolved). The theoretical MFPADs, computed in the present work for the ss-DCH and ts-DCH generation, are depicted in figures 1 and 2 for the O_2 and N_2 molecules, respectively (see legends at the bottom of the figures). The MFPADs are computed for different photoelectron kinetic energies below 40 eV (indicated for each row of panels on the left-hand site) and represent three situations, in which the incident-light polarization vector is oriented parallel or perpendicular to the molecular axis (the middle and the right columns of panels, respectively), and the average over all polarization directions (PA-MFPADs, left column of panels). It is straightforward to prove analytically that it holds: PA-MFPAD $= \frac{1}{3} \cdot$ MFPAD($\parallel$) $+ \frac{2}{3} \cdot$ MFPAD($\perp$).
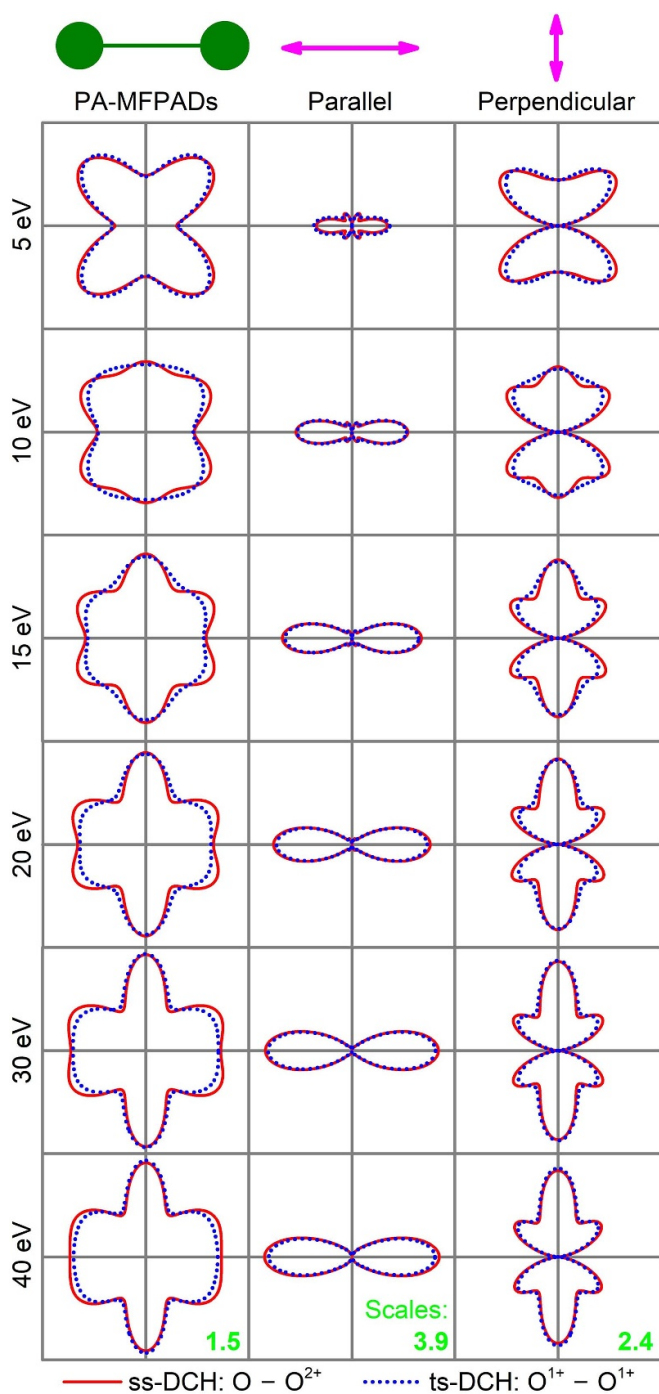
Figure 1. Normalized molecular-frame angular distributions (see text for details), computed in the present work for the secondary photoelectrons emitted during the ss-DCH (red solid curves) and ts-DCH (blue dotted curves) generation of O_2 at different photoelectron kinetic energies (indicated on the left-hand site of each row of panels). The molecule is oriented horizontally and the distributions are averaged over the left and right emitting oxygen atoms (delocalized emitting site scenario). The left column of panels depicts PA-MFPADs, while MFPADs representing parallel ($\parallel$) and perpendicular ($\perp$) orientations of the light polarization with respect to the molecular axis are shown in the middle and right columns, respectively (see also inset on the top of this figure). All panels in each column have equal relative scales. However, for a better comparison, every column has an individual relative scale, as indicated in the last row of panels by respective scale factors in green (can be considered as an absolute horizontal and vertical scales of the squared panel).
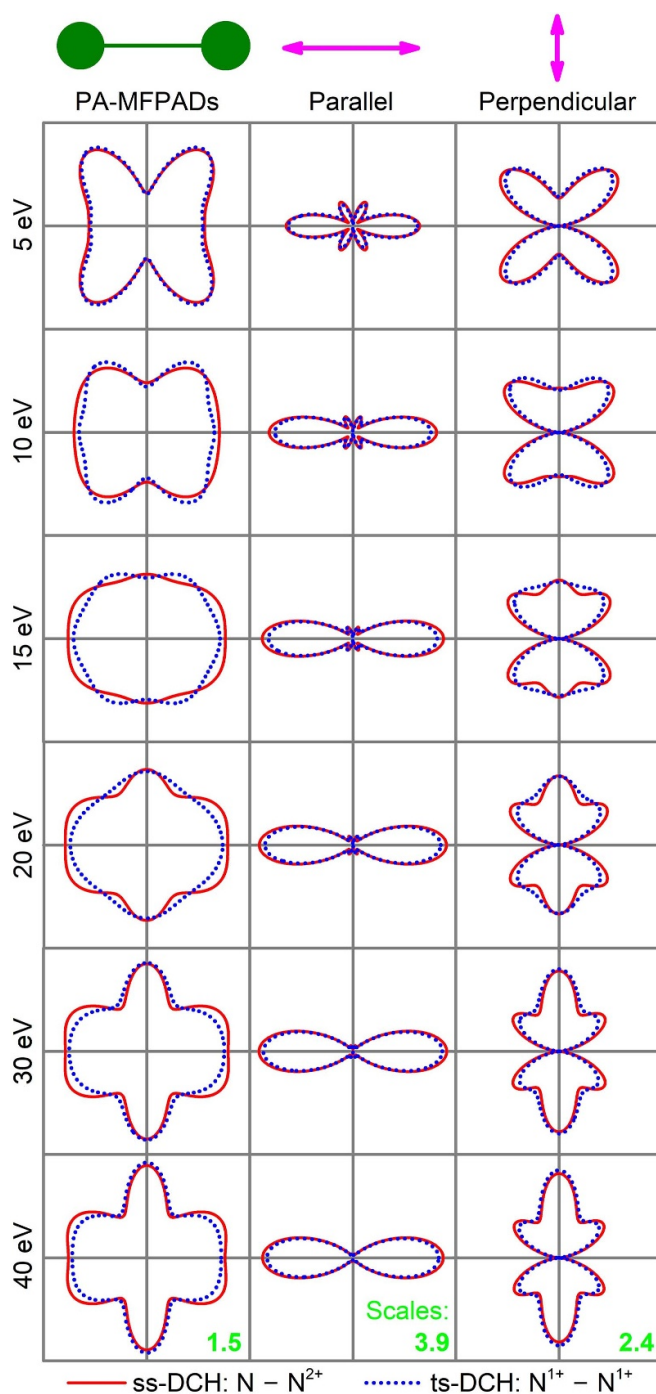
Figure 2. The same as in figure 1 but for N_2 molecules (see caption of figure 1 for details on data representation).

To enable a direct comparison, the three MFPADs of the ss-DCH (and separately those of the ts-DCH states) were normalized for each photoelectron kinetic energy (i.e. in each row of panels) to their total integral emission distribution of the respective PA-MFPAD, i.e. to the value of $\sigma_\varepsilon = \int [\int \sigma_\varepsilon(\beta,\theta) \sin\beta\, d\beta] \sin\theta\, d\theta$. Finally, for a better data representation, each column has its own relative scale for all panels. These respective scale factors are indicated in the bottom row of panels, and they represent absolute sizes of the squared panels.

J. Phys. B: At. Mol. Opt. Phys. **56** (2023) 195003

D V Rezvan *et al*

By inspecting the first columns of figures 1 and 2, one can see that the normalized PA-MFPADs of the ss-DCH and ts-DCH states of each molecule and each considered photoelectron kinetic energy have very similar shapes. Quantitatively, they differ from each other by less than 10%, and it is difficult to resolve such a small difference in an experiment. Even a differentiation of the emission distributions by considering particular mutual orientations of the molecular axis and polarization vector of the incident light (the middle and right columns of panels in figures 1 and 2) would not help to distinguish experimentally these two very different situations. Indeed, in the case of the ss-DCH, the secondary photoelectron feels two positive charges being located on the same site, and for the ts-DCH on two different sites of a molecule. Since this significant difference in the electron potentials is not notably reflected in the MFPADs computed for the delocalized emitting site scenario, one can conclude that the form of the emission distributions is governed here solely by an interference between multiply-scattered photoelectron waves.

Comparison of the MFPADs computed for the O_2 and N_2 molecules confirms this fact. Indeed, such an interference is sensitive to the phase difference between direct and scattered waves [26, 33, 35], which is proportional to the product of the photoelectron momentum $k = \sqrt{2\varepsilon}$ and the internuclear distance R. Since the bond length of O_2 molecules is by about 10% longer than that for N_2 (1.208 vs. 1.098 Å, respectively [36]), the distributions computed for these two molecules are rather similar if one compares them at different photoelectron kinetic energies: somewhat smaller energies for O_2 with somewhat larger ones for N_2. This is clearly seen from the right columns of figures 1 and 2, where the MFPAD($\perp$) for O_2 at 10 eV is similar to that of N_2 at 15 eV, or the MFPAD($\perp$) for O_2 at 20 eV is similar to that of N_2 at 30 eV.

The situation changes, if one considers a localized emitting site scenario, as was suggested in [20]. The respective MFPADs, computed for the right emitting atom of the O_2 and N_2 molecules, are depicted in figures 3 and 4, respectively. Note that for the ss-DCH, the first core-hole state was created on the right atom, whereas for the ts-DCH on the left. Mirroring these MFPADs along the horizontal direction ($L \leftrightarrow R$), generates the respective MFPADs for the left emitting atom, and an incoherent addition of those for the right and left emitters together results in the MFPADs depicted in figures 1 and 2. Figures 3 and 4 demonstrate that, similarly to the delocalized emitting site scenario, the shapes of the MFPADs computed for the ss-DCH and ts-DCH states are rather similar, confirming the fact that these distributions are governed by the multiple-scattering interference effects. An additional argument in favor is that, in the considered kinetic energy range, the computed MFPADs($\parallel$) in the second columns of figures 3 and 4 exhibit a dominant photoemission in the direction opposite to the neighbor (to the right) – the so-called backward scattering peak, which is enhanced owing to the interference between the direct and scattered waves [33].

Figures 3 and 4 demonstrate a notable quantitative difference between the MFPADs computed for the ss-DCH and ts-DCH states, and such a difference, of the order of 20%–40%, could be resolved in experiments. In particular, the ts-DCH
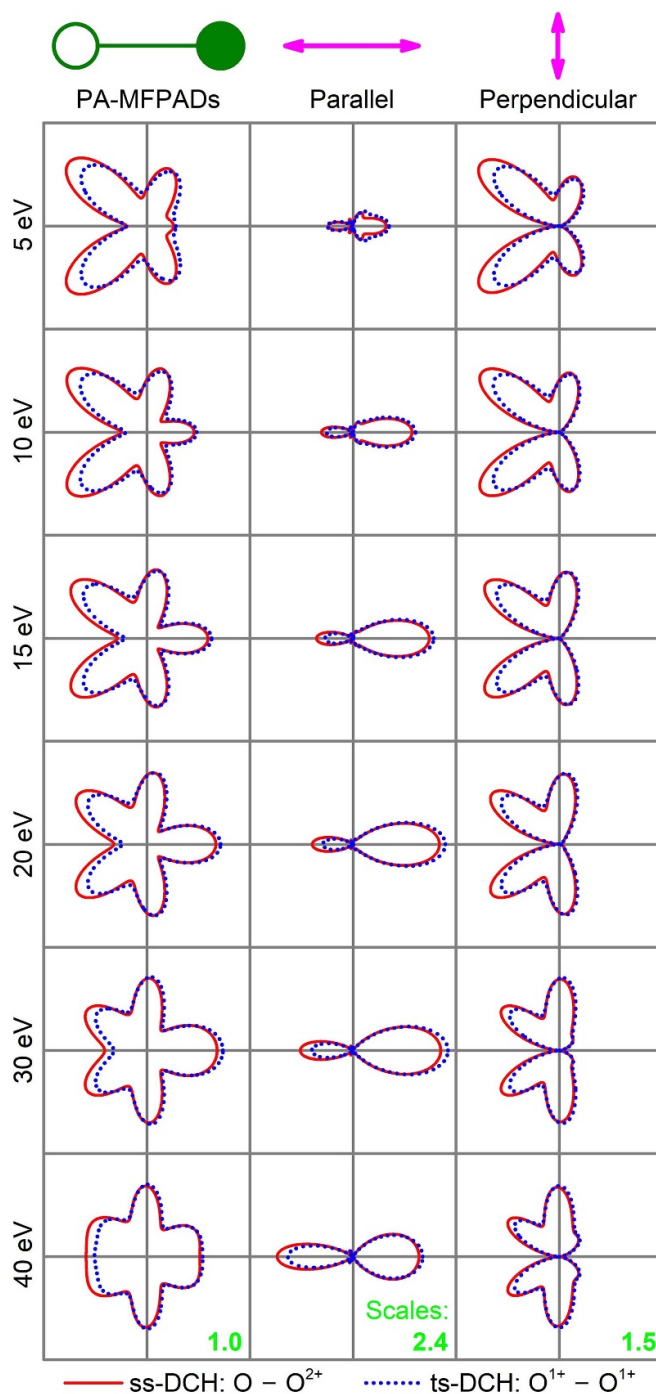

Figure 3. The same as in figure 1 but only for the right emitting oxygen atom (localized emitting site scenario), as indicated by the solid green circle on the top of this figure (see caption of figure 1 for details on data representation).

MFPADs are substantially suppressed on the left and slightly enhanced on the right emission sites (as compared to the ss-DCH MFPADs). Such a sizable enhancement and suppression of the ts-DCH MFPADs as compared to the ss-DCH ones cancels out almost completely on average of the two emitting sites. It, thus, cannot be observed for the delocalized emitting site scenario in figures 1 and 2. Although the discussed effect is caused by the significant difference in the relaxed-core ionic
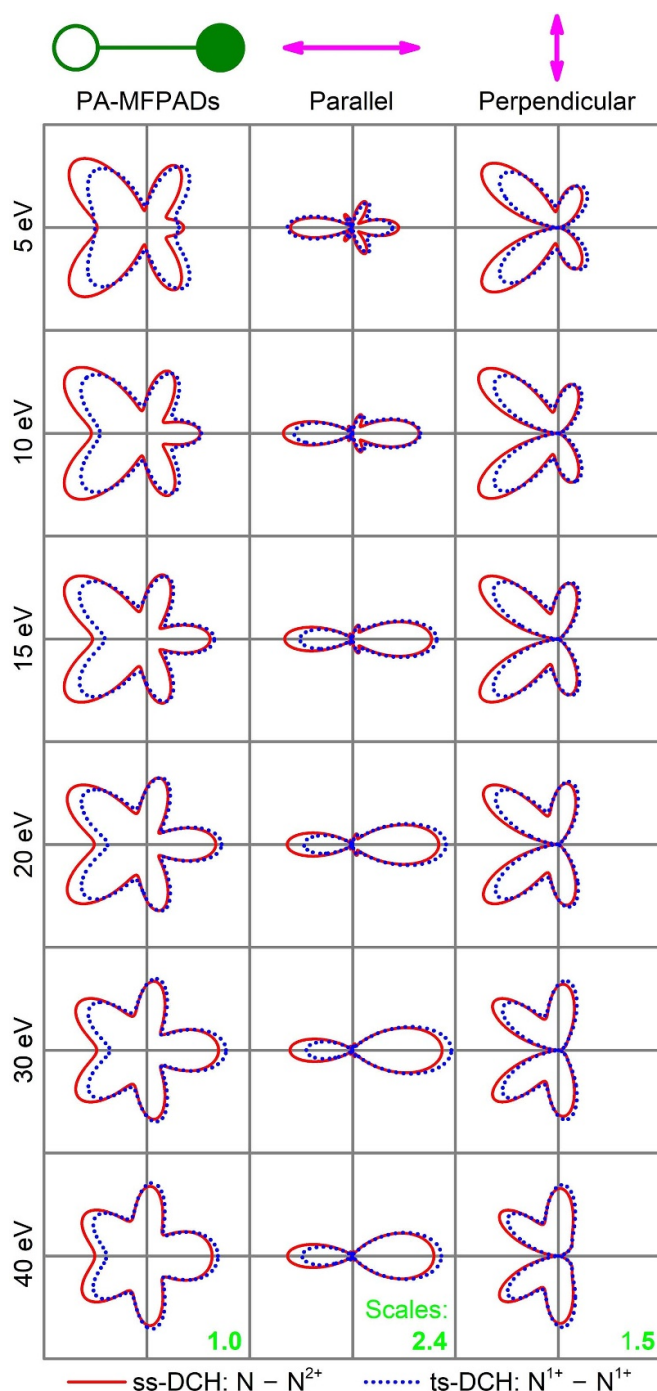
J. Phys. B: At. Mol. Opt. Phys. **56** (2023) 195003

D V Rezvan *et al*

Figure 4. The same as in figure 3 but for N_2 molecules (see captions of figures 1 and 3 for details on data representation).

potentials, generated by the DCH states for secondary photoelectrons, the effect is moderate, even in the localized emitting site scenario. As suggested above, this might be caused by a dominant role of the multiple-scattering interference effects.

4. Summary

Molecular-frame angular distributions of the secondary photoelectrons emitted during the single-site and two-site DCH

generation in the homonuclear O_2 and N_2 molecules are computed in a systematic way for different photoelectron kinetic energies, mutual orientations of the molecular axis and polarization of the incident light, and, in particular, different emitting atomic site localization scenarios. The calculations are performed with the SC method in the relaxed-core Hartree–Fock approximation. The considered kinetic energy interval below 40 eV is found to be free of any shape resonances for both molecules, which justifies reliability of the used one-particle approximation. The present theoretical results suggest that the studied emission distributions are mainly governed by multiple-scattering interference effects, and the substantial difference in the ionic potentials generated by the ss-DCH and ts-DCH states is not prominently manifested in the computed MFPADs. This difference, however, can be observed in the MFPADs if one compares the ss-DCH and ts-DCH distributions for the emitting atom localized on one molecular site. We hope that the present theoretical study provides a sufficient motivation for performing such systematic experiments at presently operating XFEL facilities.

Data availability statement

All data that support the findings of this study are included within the article (and any supplementary files).

ORCID iDs

Dmitrii V Rezvan ⬤ https://orcid.org/0009-0008-0420-1893
Nikolay M Novikovskiy ⬤ https://orcid.org/0000-0002-5781-1862
Boris M Lagutin ⬤ https://orcid.org/0000-0002-8247-9769
Philipp V Demekhin ⬤ https://orcid.org/0000-0001-9797-6648

References

[1] Siegbahn K *et al* 1969 *Esca Applied to Free Molecules* (North-Holland Pub. Co)
[2] Cederbaum L S, Tarantelli F, Sgamellotti A and Schirmer J 1986 *J. Chem. Phys.* **85** 6513
[3] Cederbaum L S, Tarantelli F, Sgamellotti A Schirmer J 1987 *J. Chem. Phys.* **86** 2168
[4] Ohrendorf E M-L, Cederbaum L S and Tarantelli F 1991 *Phys. Rev.* A **44** 205
[5] Ågren H and Jensen H J 1993 *Chem. Phys.* **172** 45
[6] Reynaud C, Gaveau M-A, Bisson K, Millie P, Nenner I, Bodeur S, Archirel P and Levy B 1996 *J. Phys.* B **29** 5403
[7] Schmidt V 1992 *Rep. Prog. Phys.* **55** 1483
[8] Kanter E P, Dunford R W, Krässig B, Southworth S H and Young L 2006 *Radiat. Phys. Chem.* **75** 2174
[9] Hoszowska J *et al* 2009 *Phys. Rev. Lett.* **102** 073006

J. Phys. B: At. Mol. Opt. Phys. **56** (2023) 195003

D V Rezvan *et al*

[10] Eland J H D, Tashiro M, Linusson P, Ehara M, Ueda K and Feifel R 2010 *Phys. Rev. Lett.* **105** 213005
[11] Lablanquie P *et al* 2011 *Phys. Rev. Lett.* **106** 063003
[12] Santra R, Kryzhevoi N V and Cederbaum L S 2009 *Phys. Rev. Lett.* **103** 013002
[13] Tashiro M, Ehara M and Ueda K 2010 *Chem. Phys. Lett.* **496** 217
[14] Tashiro M, Ehara M, Fukuzawa H, Ueda K, Buth C, Kryzhevoi N V and Cederbaum L S 2010 *J. Chem. Phys.* **132** 184302
[15] Takahashi O, Tashiro M, Ehara M, Yamasaki K and Ueda K 2011 *J. Chem. Phys.* A **115** 12070
[16] Cryan J P *et al* 2010 *Phys. Rev. Lett.* **105** 083004
[17] Fang L *et al* 2010 *Phys. Rev. Lett.* **105** 083005
[18] Berrah B *et al* 2011 *Proc. Natl Acad. Sci. USA* **108** 16912
[19] Salén P *et al* 2012 *Phys. Rev. Lett.* **108** 153003
[20] Kastirke G *et al* 2020 *Phys. Rev. Lett.* **125** 163201
[21] Landers A *et al* 2001 *Phys. Rev. Lett.* **87** 013002
[22] Jahnke T *et al* 2002 *Phys. Rev. Lett.* **88** 073002
[23] Williams J B *et al* 2012 *Phys. Rev. Lett.* **108** 233002
[24] Fukuzawa H *et al* 2019 *J. Chem. Phys.* **150** 174306
[25] Kaiser L *et al* 2020 *J. Phys. B: At. Mol. Opt. Phys.* **53** 194002
[26] Kastirke G *et al* 2020 *Phys. Rev. X* **10** 021052
[27] Rist J *et al* 2021 *Nat. Commun.* **12** 6657
[28] Rezvan D M, Novikovskiy N M, Martin L, Artemyev A N and Demekhin Ph V 2022 *Phys. Rev.* A **105** 033108
[29] Demekhin Ph V, Omel'yanenko D V, Lagutin B M, Sukhorukov V L, Werner L, Ehresmann A, Schartner K-H and Schmoranzer H 2007 *Opt. Spectrosc.* **102** 318
[30] Demekhin Ph V, Ehresmann A and Sukhorukov V L 2011 *J. Chem. Phys.* **134** 024113
[31] Galitskiy S A, Artemyev A N, Jänkälä K, Lagutin B M and Demekhin P V 2015 *J. Chem. Phys.* **142** 034306
[32] Novikovskiy N M, Artemyev A N, Rezvan D V, Lagutin B M and Demekhin Ph V 2022 *J. Phys. B: At. Mol. Opt. Phys.* **55** 175001
[33] Kastirke G *et al* 2022 *Phys. Chem. Chem. Phys.* **24** 27121
[34] Kircher M *et al* 2019 *Phys. Rev. Lett.* **123** 243201
[35] Vela-Pérez I *et al* 2023 *Phys. Chem. Chem. Phys.* **25** 13784
[36] Huber K P and Herzberg G 1979 *Molecular Spectra and Molecular Structure IV: Constants of Diatomic Molecules* (Van Nostrand-Reinhold)